Geophysical Research Letters

Key Points:
- The MJO is linked to significant temperature variability over North America outside of winter
- Peaks in MJO covariability with temperature occur outside of winter for much of North America
- The MJO contributes to predictive skill of North American temperatures in spring, summer, and fall

Correspondence to:
A. M. Jenney,
andrea@atmos.colostate.edu

The Seasonality and Regionality of MJO Impacts on North American Temperature

A. M. Jenney[1] ⓘ **, K. M. Nardi**[1] ⓘ **, E. A. Barnes**[1] ⓘ **, and D. A. Randall**[1]

[1]Department of Atmospheric Science, Colorado State University, Fort Collins, CO, USA

Abstract It is widely accepted that the Madden-Julian Oscillation's (MJO) influence on North American temperature is strongest in winter. A growing body of literature demonstrates that the MJO also influences North American weather in other seasons. Here we use observations to investigate the seasonality and regionality of the MJO's impact on weather station daily maximum air temperature over North America (NA). Consistent with previous work, we find the strongest MJO signal in temperatures over eastern NA and Alaska during winter. However, the peak MJO signals over much of central NA, western NA, and south Texas occur outside of winter. We investigate how this translates to forecast skill and conduct leave-one-out cross-validated empirical forecasts of maximum surface air temperature using the phase of the MJO and lead time as predictors. Our results suggest the potential for more skillful long-range forecasts of weather over NA during spring, summer, and fall.

Plain Language Summary Large, organized storms in the tropical Indian and West Pacific Oceans can excite waves in the atmosphere that influence weather over North America. Much of our understanding of this process focuses on the northern winter season, but we show evidence that for some parts of North America the storms also influence daily maximum temperature during spring, summer, or fall. Our results suggest the potential for more skillful long-range forecasts of North American weather during spring, summer, and fall.

1. Introduction

Forecasts of weather at subseasonal-to-seasonal (S2S) time scales are useful to a wide range of societal sectors (White et al., 2017). Skillful S2S forecasts have the potential to save lives and money. However, the chaotic nature of the atmosphere makes deterministic forecasts beyond about 10 days a challenge. Skill at extended lead times comes from slowly varying systems such as the ocean, land surface, and low-frequency atmospheric phenomena such as the Madden-Julian Oscillation (MJO) and the stratospheric Quasi-Biennial Oscillation. Efforts are underway to utilize these slowly varying weather systems to improve forecasts. While S2S forecasts remain a challenge, there is evidence that improvements to extended-range forecasts are possible (e.g., Johnson et al., 2014; Mundhenk et al., 2018; Rodney et al., 2013).

The MJO, a large eastward propagating tropical convective system, is considered to be one of the most important sources of predictive skill at S2S time scales (Zhang, 2013). The dipole of anomalous divergence and convergence at the level of convective outflow associated with the MJO makes it a very efficient source of tropical Rossby waves (Lin, 2009; Sardeshmukh & Hoskins, 1988; Seo & Son, 2012; Seo et al., 2017; Tseng et al., 2019). MJO-excited Rossby waves have been linked to variability and predictability of the extratropical circulation (e.g., Black et al., 2017; Cassou, 2008; Henderson et al., 2016; Higgins & Mo, 1997; Guo et al., 2017; Kang & Tziperman, 2018; Lin, Brunet, & Fontecilla, 2010; Moore et al., 2010; Mori & Watanabe, 2008; Seo & Son, 2012; Zheng et al., 2018), precipitation (e.g., Curtis, 2017; DelSole et al., 2017; Jenney et al., 2019; Jones et al., 2011; Lin, Brunet, & Mo, 2010; Zheng et al., 2018), atmospheric rivers (Baggett et al., 2017; Mundhenk et al., 2018), and temperature (e.g., Barrett, 2019; Jenney et al., 2019; Johnson et al., 2014; Lee & Grotjahn, 2019; Matsueda & Takaya, 2015; Rodney et al., 2013; Zheng et al., 2018).

The influence of the MJO on extratropical weather is best established for the boreal winter season (Stan et al., 2017). The results from winter studies do not necessarily extend to other seasons because Rossby wave generation and propagation are very sensitive to the background-state winds (Bladé & Hartmann, 1995; Henderson et al., 2017; Hoskins & Ambrizzi, 1993; Newman & Sardeshmukh, 1998; Sardeshmukh & Hoskins, 1988; Simmons et al., 1983; Ting & Sardeshmukh, 1993). In the Northern Hemisphere, stronger

background winds support stationary waves with longer wavelengths and allow a wider range of Rossby wavelengths to propagate poleward before being absorbed or reflected. In addition, the MJO's propagation changes with the seasonal cycle, exhibiting a northward component during boreal summer (e.g., Wang & Rui, 1990).

Better nonwinter forecasts on S2S time scales can be useful to decision makers because many high-impact extreme events such as floods and heat waves can occur during the warm season. For example, the agricultural sector is one of the largest consumers of meteorological information, and many important agricultural applications of weather forecasts occur during spring and summer (White et al., 2017).

There is increasing evidence that the MJO influences the extratropical circulation outside of boreal winter. Wang et al. (2013) estimate that at least 20% of extratropical intraseasonal variability over the North Pacific in summer is excited in the tropics. Moon et al. (2013) locate hot spots along the Northern Hemisphere jet stream where summer variability is linked to the MJO. The MJO has been linked with summer precipitation over Mexico (Mo, 2000) and that associated with the North American monsoon (Lorenz & Hartmann, 2006; Mo, 2000). Additionally, the state of the spring and early summer MJO has been shown to offer predictive skill for severe weather over parts of North America (Baggett et al., 2018).

Given the desire for improved forecasts of weather at S2S time scales, and their potential to save lives and money, it is important to understand more completely how the MJO affects the extratropical circulation and surface weather in seasons other than boreal winter. Studies designed to look deeper into this question have typically relied on the use of lagged composite maps (e.g., Bond & Vecchi, 2003; Curtis & Gamble, 2016; Donald et al., 2006; Matsueda & Takaya, 2015; Moon et al., 2013; Zhou et al., 2012). Many such maps are needed because of the many phase and lag combinations, which ultimately restricts their utility for understanding the regionality and seasonality of MJO teleconnections over many lead times and MJO phases. We utilize the STRIPES (Sensitivity to the Remote Influence of Periodic Weather EventS) index (Jenney et al., 2019) as an alternative method to investigate the seasonality and regionality of MJO impacts on temperature over North America. In addition, we show that for some regions the predictive skill offered by the MJO is strong in seasons other than winter. This can guide the search for predictive skill at S2S time scales.

2. Data and Methods

2.1. Observed MJO Impacts

We use daily data from January 1980 to August 2018. We quantify the position and strength of the MJO using the outgoing longwave radiation MJO Index (OMI; Kiladis et al., 2014). We choose this index because its definition varies smoothly with the calendar year and can thus capture the seasonality of the MJO teleconnection while also taking into account the seasonality of the MJO itself. The OMI has been shown to accurately represent the propagation of the MJO in both summer and winter (Wang et al., 2018). In composites, and in the calculation of the STRIPES index, we consider only MJO days with an OMI amplitude ($\sqrt{PC_1^2 + PC_2^2}$) greater than 1.0.

We use weather station daily temperature maxima from the Global Historical Climatology Network-Daily database (Menne et al., 2012). Only North American stations with daily maximum temperature time series that are at least 50% complete for at least 50% of the years in the time period are used, leaving 8,356 weather stations (Figure 1a). Data are converted to anomalies by removing the first three annual harmonics and long-term mean.

The observed sensitivity of temperature to the MJO is quantified using the STRIPES index (Jenney et al., 2019), which condenses the information contained in a lagged composite of a variable across a range of lags and phases. The STRIPES index itself does not directly communicate information about the phase dependency of MJO teleconnections but captures this dependency through explicit quantification of the magnitude of the component of the lagged composite that is consistent with MJO propagation (see Jenney et al., 2019). Hence, the STRIPES index is large when the covariability of the variable with the MJO is strong and there is consistency between MJO events. Its value can be understood as the average magnitude of the composite response of that variable conditioned on the MJO. We assume that the MJO spends between 5 and 7 days in each of the eight phases, reorder the phases, and consider lags 0 to 42 days after each phase. For the calculation of the average STRIPES index over multiple weather stations, we first apply an area weighting as in McKinnon et al. (2016) to construct a single time series for the region, so that areas with higher densities of weather stations are not overweighted.
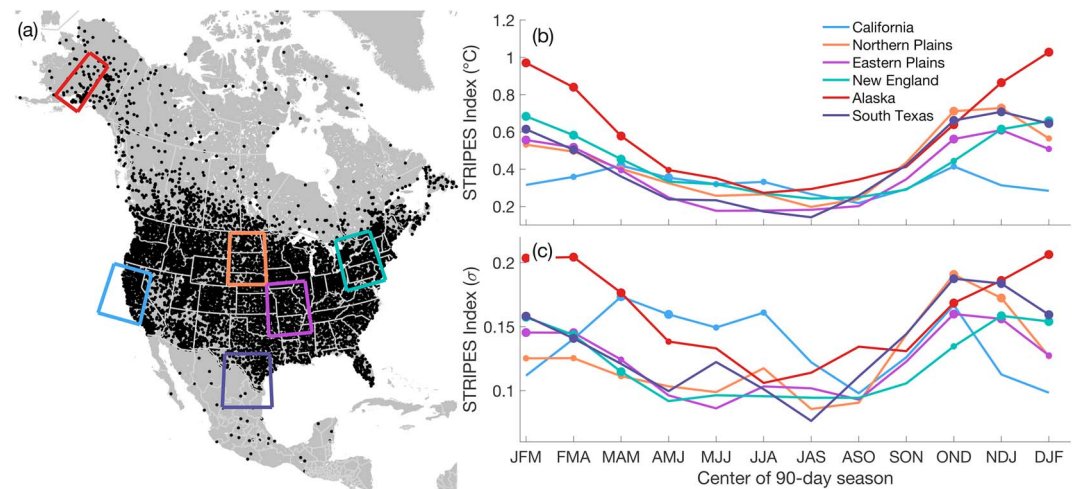
Figure 1. Seasonality of the Madden-Julian Oscillation teleconnection for daily maximum temperature at weather stations between January 1980 and August 2018. (a) Black points show the location of weather stations that meet our data completeness requirements (see text). Colored boxes enclose regions for which the STRIPES index is calculated. (b) The STRIPES index for each region in units of degrees Celsius and (c) standard deviations. Large (small) circles indicate significance at $\alpha < 0.05$ ($\alpha < 0.10$). STRIPES = Sensitivity to the Remote Influence of Periodic Weather EventS. FMA = February–April; MAM = March–May; AMJ = April–June; MJJ = May–July; JJA = June–August; JAS = July–September; ASO = August–October; SON = September–November; OND = October–December; NDJ = November–January; DJF = December–February.

We calculate significance of the STRIPES index using a bootstrap method with 500 samples. For each bootstrap sample, we calculate the STRIPES index using a distribution of MJO days that have the same month and day as the MJO days used in the analysis, but with a randomly sampled (with replacement) year. This allows the time of year and memory between MJO phases, which occur as sequences of consecutive days, to be retained. We show significance at $\alpha < 0.10$ and $\alpha < 0.05$, which are taken to be the 90th and 95th percentiles of the distribution of STRIPES indices created by the bootstrapping method.

2.2. Forecast Skill

To make forecasts of temperature (either above or below normal), we apply an empirical prediction scheme. This method was first introduced by Johnson et al. (2014) and later applied by Mundhenk et al. (2018) and Baggett et al. (2018). It produces weekly (5-day running mean) temperature forecasts out to 42 days based only on the current active state of the MJO. To make a forecast, the scheme generates a conditional temperature anomaly distribution based on the phase of the MJO at initialization (assuming an active MJO) and the number of days after initialization. If the median of this conditional distribution is greater (less) than the median of the full climatological distribution of temperature for the season, the scheme forecasts above- (below-) normal temperatures. We apply the model to 12 overlapping 3-month seasons (e.g., December–February [DJF] and January–March; Baggett et al., 2018). Unlike Johnson et al. (2014), we do not use any other predictors along with the MJO (e.g., the state of the El Niño–Southern Oscillation).

For forecasts, we use data from the period 1979–2017. The temperature data used are the daily maxima of 6-hourly near-surface air temperatures from the National Center for Environmental Prediction/National Center for Atmospheric Research Reanalysis 1 (Kalnay et al., 1996), which are then smoothed to weekly values by applying a 5-day centered running mean. We make forecasts with this data set because it is currently utilized in operations and research by the National Oceanographic and Atmospheric Administration's Climate Prediction Center, a major stakeholder in S2S forecasting. All forecasts are made for area averages over $7.5° \times 7.5°$ regions. MJO activity is quantified using the real-time OMI index of Wang et al. (2019), and we construct conditional distributions using only active MJO days with a real-time OMI amplitude of 1.0 or greater. At this threshold, forecasts can be made about 55% of the time.

We employ a leave-one-year-out cross-validation method to calculate forecast skill (Baggett et al., 2018; Johnson et al., 2014; Mundhenk et al., 2018). To accomplish this, we make a forecast for a particular season during a particular year using all seasons/years except the one we are validating. Skill is quantified using the
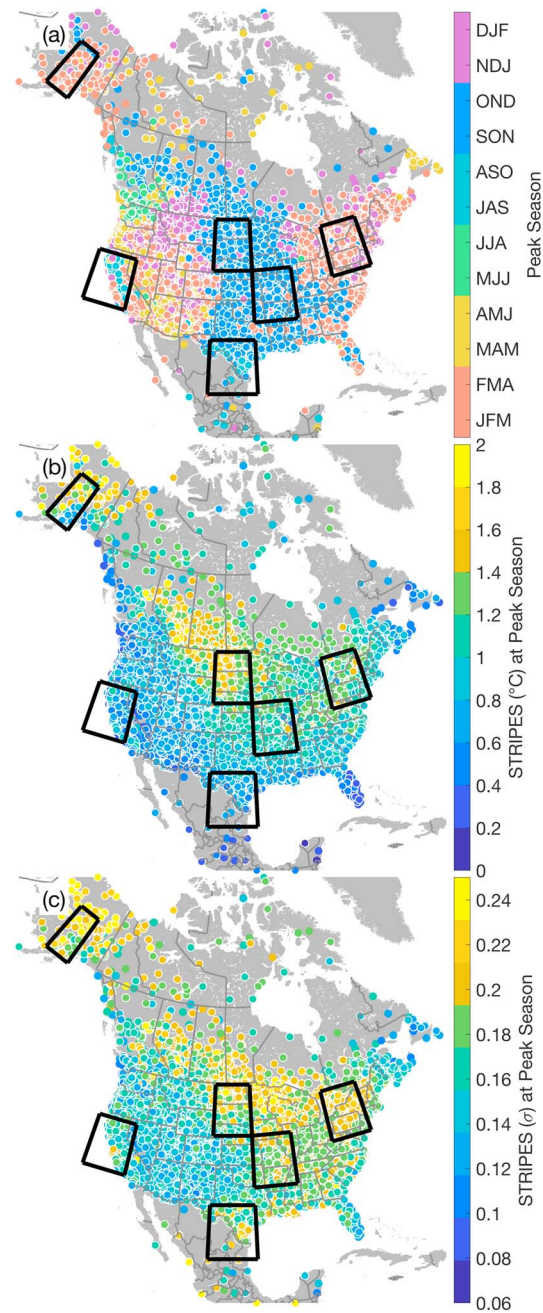
Figure 2. (a) Season of the peak significant value of the STRIPES index (in standard deviations, σ) for daily precipitation totals at weather stations, (b) the magnitude of that maximum in degrees Celsius, and (c) σ. Regions highlighted in Figure 1 are enclosed with black boxes. Only weather stations with significant peaks at $\alpha < 0.10$ are plotted. Weather stations whose peaks are significant at $\alpha < 0.05$ are enclosed with white circles. STRIPES = Sensitivity to the Remote Influence of Periodic Weather EventS. JFM = January–March; FMA = February–April; MAM = March–May; AMJ = April–June; MJJ = May–July; JJA = June–August; JAS = July–September; ASO = August–October; SON = September–November; OND = October–December; NDJ = November–January; DJF = December–February.

AGU
100
ADVANCING EARTH
AND SPACE SCIENCE

Geophysical Research Letters

10.1029/2019GL083950

same Heidke skill score (HSS) used in Mundhenk et al. (2018; see also Wilks, 2011). For reference, a HSS of 0 (33) implies that the model is correct as often (twice as often) as incorrect.

3. Results

3.1. Observed MJO Links

Because the STRIPES index is a single number for a region or point, it is easy to plot its variations over time and space. Figure 1 shows the annual variation of the STRIPES index for weather station daily maximum temperature for various North American regions (colored boxes). Each region was selected for one or more of the following reasons: The region has previously been linked with the MJO; inclusion of the region will help to create a geographically diverse set of regions that cover areas with societal importance; and/or because the weather stations within the region agree in their timing and magnitude of their sensitivity to the MJO (Figure 2). To investigate the seasonality of the apparent MJO teleconnections at weather stations, we calculate the STRIPES index for overlapping 3-month seasons using the time series for each area-averaged region. Figure 1b shows that for the selected regions the average magnitude of the apparent significant winter MJO impact on temperature is between about 0.6 and 1 °C (i.e., the STRIPES index). The apparent MJO teleconnection during summer appears to be weaker for all six regions, with most regions showing STRIPES indices around 0.2 °C, and not indicating any significance. This is consistent with previous results that indicate stronger MJO impacts on North American temperature in boreal winter (Zhou et al., 2012).

Figure 1b shows that MJO teleconnections to the extratropics are strongest in the winter (DJF) for Alaska and New England. This is consistent with previous work; these are both centers of action of the Pacific-North America pattern, a quasi-stationary feature of the local large-scale circulation that is tied to the MJO (Goss & Feldstein, 2015; Mori & Watanabe, 2008; Seo et al., 2017), and most active during the winter months (Barnston & Livezey, 1987). However, other regions show significant peaks in MJO covariability outside of DJF. Temperature over the northern plains, eastern plains, and south Texas regions display peaks in MJO covariability during October–December (OND) and November–January (NDJ), 30–60 days prior to DJF. The California region has a weaker but significant peak during OND, with comparable peaks in late spring and early summer.

Figure 1c shows the STRIPES index normalized so that it is in units of standard deviations, σ. Each region and season is standardized independently. This standardized STRIPES index shows the magnitude of the covariability of station-based surface temperatures with the MJO relative to the local seasonal variance of temperature, which is relatively high (low) over land in the extratropical winter (summer). From here on, we discuss the STRIPES index in "standardized" units of σ, because our focus is on the seasonality and regionality of the MJO teleconnection from a weather prediction perspective—a 1 °C departure from climatology is less common in seasons and regions where the variability of temperature is small. There is little change in the timing of maxima and minima of the STRIPES index from degree Celsius to σ units. Although there are slight (not more than 1 month) shifts in the exact 3-month season when the peak MJO signal occurs for some regions, the general shape of the seasonality of the MJO signal for each region is preserved. For example, the northern plains maintains the strongest signal in late fall, with a minimum in summer, despite the peak signal moving from the NDJ season to the OND season. However, non-DJF peaks for some regions now appear to scale with other regions' winter peaks. In σ units, the magnitude of the influence of the MJO on the three regions for which impacts peak in November/December is comparable to that for winter over Alaska and New England, which are two regions understood to be strongly influenced by the MJO (Zheng et al., 2018; Zhou et al., 2012). The seasonality of the strength of MJO impacts on temperature for the California region is particularly interesting. While spring and summer peaks are apparent in Figure 1b, they appear small relative to the winter peaks of Alaska because of the relatively small local temperature variance over this region in summer. However, Figure 1c shows that in σ units California's spring and summer sensitivity of temperature to the MJO scales with that for fall and winter in other regions. In earlier work, the MJO has been shown to be linked with summer heat waves over the California Central Valley (Lee & Grotjahn, 2019). Here we show that the peak influence of the MJO on daily temperature maxima over this region occurs during spring and summer.

To investigate the seasonal sensitivity of local temperature—that is, temperature at points, rather than the mean temperature over a large region—to the MJO, we apply the STRIPES index to individual weather stations for each overlapping season. Figure 2a shows the season where the peak STRIPES index occurs (in σ) for daily temperature maxima. Only weather stations with a significant (at $\alpha < 0.10$) STRIPES index during
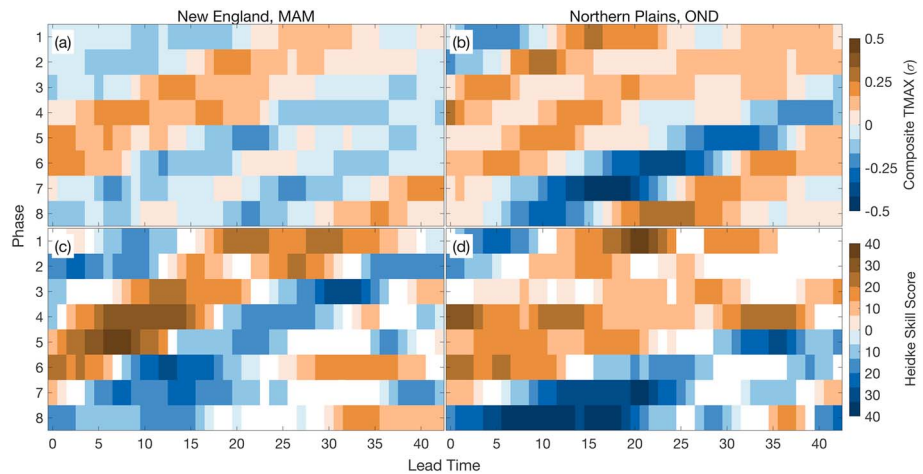
Figure 3. (a) Composite weather station daily maximum temperature and (c) HSS for predictions of surface air temperature during MAM in the New England region shown in Figures 1 and 2. (b, d) As in (a) and (c) but during OND over the northern plains. For HSS, orange (blue) colors indicate a forecast for above (below) average temperatures. HSS values below 0 (poor skill) are indicated in white. HSS = Heidke skill score; MAM = March–May; OND = October–December.

the peak season are plotted, and weather stations for which $\alpha < 0.05$ are marked by white circles. Despite some inhomogeneity, there is generally good spatial agreement in the peak sensitivity of temperature to the MJO, with coherent regions emerging. Much of Alaska and New England display the strongest MJO signal during the latter half of boreal winter. A large region over the Great Plains experiences peak MJO impacts during fall. There are even some areas with summer peaks, such as northern Washington and southern British Columbia, the California Central Valley, and the southern tip of Texas.

At this station-based spatial scale, Alaska and eastern North America (excluding the easternmost portion of Canada) show the strongest sensitivities (in σ, Figure 2c) of temperature to the MJO, consistent with previous work (Baxter et al., 2014; Jenney et al., 2019; Johnson et al., 2014; Matsueda & Takaya, 2015; Schreck et al., 2013; Zheng et al., 2018; Zhou et al., 2012). These regions display their peaks in fall and winter.

3.2. Tying Observed MJO Covariability to Forecast Skill

Thus far we have demonstrated that the MJO is linked to variability in surface temperature in seasons other than winter. This suggests that the MJO may offer predictive skill in seasons outside of winter. We now demonstrate that this is actually the case, by using the empirical model described above and used by Johnson et al. (2014), Mundhenk et al. (2018), and Baggett et al. (2018).

We select two regions and seasons outside of winter to highlight how the MJO links with forecast skill. Figure 3a is a lagged composite of daily maximum temperature for weather stations in the New England region shown in Figures 1 and 2, and for the March–May season. Diagonal stripes of composites of the same sign that have a slope consistent with the MJO propagation speed are suggestive of a physical link between the MJO and temperature over that region (Baggett et al., 2017; Jenney et al., 2019; Mundhenk et al., 2018). Figure 3c shows the HSS for the same region, season, and phase and lag combinations, but for gridded reanalysis surface air temperature. Positive HSS values are shown with colors and indicate good skill, and negative HSS values indicating poor skill are shown as white. The colors represent the sign of the temperature forecast made (above or below normal). Comparison between the HSS and temperature composite shows that stripes of positive skill align well with the stripes of composited temperature. This implies that, for this region and season combination, there is a strong MJO signal in observed temperature variability and that the signal translates to high forecast skill using just the MJO as a predictor. Figures 3b and 3d show similar results for the OND season over the northern plains region and demonstrates that not only does the MJO covary with temperature, but it is also a source of predictive skill for the temperature in this region. Many factors can influence forecast skill. Here, high skill indicates high sign consistency among members of the distribution of observed anomalous surface air temperatures created by conditioning on an MJO phase and lead time. For a combination of a particular phase and lead time, synoptic weather noise or random chance may contribute to a high HSS. However, we can be confident that forecast skill is attributable
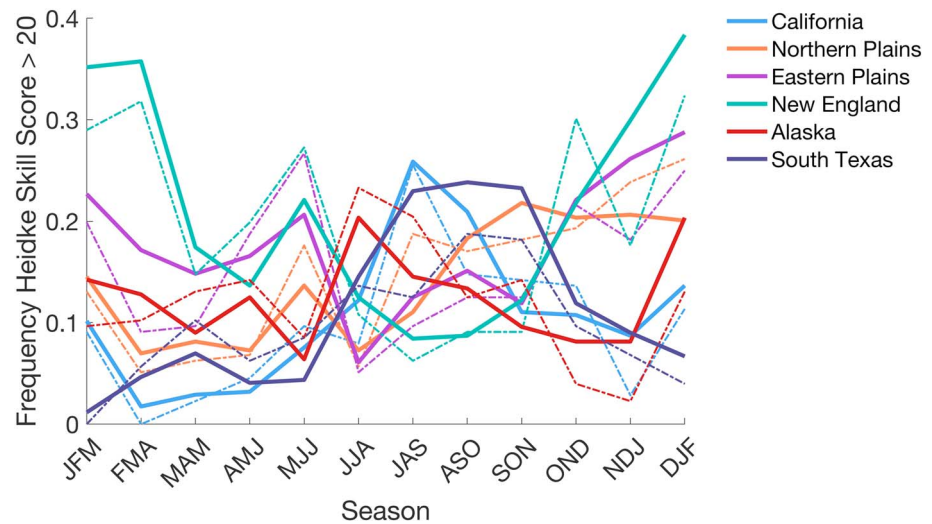
Figure 4. Fraction of forecasts that have a Heidke skill score >20 considering all phase and lead time combinations (solid lines) and for lead times at subseasonal-to-seasonal time scales of 14 to 35 days (dash-dotted lines) for the same regions as those shown in Figures 1 and 2, and for 12 overlapping 3-month seasons. FMA = February–April; MAM = March–May; AMJ = April–June; MJJ = May–July; JJA = June–August; JAS = July–September; ASO = August–October; SON = September–November; OND = October–December; NDJ = November–January; DJF = December–February.

to the influence of the MJO because good skill exists for multiple phase and lag combinations and because this skill appears as diagonal stripes in Figures 3c and 3d. We now discuss the seasonality and regionality of forecast skill for MJO impacts on surface temperature. Figure 4 shows the fraction of forecasts that have a HSS > 20 for all phase and lag combinations (up to a lead time of 42 days), for 12 overlapping 3-month seasons. Also shown is the same but for lead times relevant for S2S forecasts (14 to 35 days). A threshold of 20 corresponds to 1.5 correct forecasts for every incorrect forecast. We choose this threshold based on a significance test of HSS using the "random walk" method of DelSole and Tippett (2016). About 90% of HSS at or above 20 are significant ($\alpha < 0.05$) for all seasons in the regions considered. However, we find that the seasonality of skill is not very sensitive to the choice of HSS threshold (not shown). Like the observed MJO impact on surface temperature, there is substantial seasonality in forecast skill, with four of the six selected regions showing skill peaks in seasons outside of winter. Comparison between Figures 1c and 4 shows some agreement of the seasonality of observed MJO covariability and the seasonality of forecast skill. For New England, the MJO best predicts anomalous near-surface air temperature during the winter months, which is consistent with the seasonality of the observed sensitivity of temperature to the MJO. The northern plains shows good skill occurring during the fall, which is when the largest STRIPES index (σ) occurs. Interestingly, the minimum of the MJO's ability to skillfully predict temperature for this region occurs during the late winter, when the observed MJO signal on temperature is only moderately weak but significantly detectable. Over the California region, peak skill occurs during the late summer, consistent with previous work linking heat waves over the region to antecedent MJO activity (Lee & Grotjahn, 2019). The spring peak in skill for the eastern plains may be particularly useful to a range of sectors as this season is associated with elevated heat wave risk (Kalkstein & Smoyer, 1993) and the onset of the growing season. The skill shown here is for empirical predictions of temperature using just the MJO as a predictor. Many other factors could also influence the seasonality of prediction skill. Here we show that the MJO provides skill in seasons outside of winter.

4. Discussion and Conclusions

The influence of the MJO on extratropical weather is best established for the boreal winter season (Stan et al., 2017). However, a growing body of literature demonstrates that the MJO influences weather in other seasons (Baggett et al., 2018; Curtis, 2017; Lorenz & Hartmann, 2006; Mo, 2000; Moon et al., 2013; Wang et al., 2013). Here we show that, for near-surface air temperature over North America, the MJO's impacts on both observed variability and forecast skill displays substantial seasonality and regionality. We find the

MJO covaries with and contributes to forecast skill of near-surface air temperature over a large portion of North America outside of the DJF winter season.

We have also shown sensitivity of the apparent MJO signal in surface air temperature to standardization by local and seasonal variance. Standardization does not strongly influence the timing of peak MJO impacts. Many previous studies quantify MJO impacts through composite methods in which standardization is not used. Because of the strong cold-season variability of extratropical geopotential heights and temperatures, composites made for winter will generally have stronger magnitudes than those made for summer. However, our interest in the MJO's impacts on North American temperature is rooted in a desire to improve forecasts on S2S leads. A 1 °C departure in temperature is more abnormal and may have a higher impact over a region and/or during a season for which the temperature variance is very low. In other words, a 1 °C departure from average over a region or during a season where the standard deviation of temperature is very small is more extreme than a similar departure of temperature for a region or season where the standard deviation of temperature may be multiple degrees Celsius, and for which such a temperature anomaly is more common. We are interested in departures of the temperature from what is considered normal for that season or region. This allows seasons and regions to be compared.

Our detection of strong nonwinter observed covariability of North American temperatures with the MJO is aided by three factors. First, we use the STRIPES index rather than lagged composite maps or correlation/covariance maps. This allows for the easy identification of peaks in MJO covariability at individual locations throughout the seasonal cycle. Second, we use the OMI index to define the state of the MJO, rather than the more commonly used Real-time Multivariate MJO index (Wheeler & Hendon, 2004). Wang et al. (2018) show that the Real-time Multivariate MJO and OMI indices differ greatly in their ability to capture the propagation of the MJO, particularly in the boreal summer. Finally, we normalize the temperature variability by the seasonally and regionally varying standard deviation of the temperature to remove the sensitivity of the MJO signal to climatological variance.

Our work demonstrates that the MJO's impacts on surface temperature over North America vary seasonally and regionally and that this translates to a similar seasonality and regionality of the MJO's utility as a predictor on S2S time scales.

References

Baggett, C. F., Barnes, E. A., Maloney, E. D., & Mundhenk, B. D. (2017). Advancing atmospheric river forecasts into subseasonal-to-seasonal time scales: Forecasting ARs at S2S time scales. *Geophysical Research Letters*, *44*, 7528–7536. https://doi.org/10.1002/2017GL074434

Baggett, C. F., Nardi, K. M., Childs, S. J., Zito, S. N., Barnes, E. A., & Maloney, E. D. (2018). Skillful subseasonal forecasts of weekly tornado and hail activity using the Madden-Julian Oscillation. *Journal of Geophysical Research: Atmospheres*, *123*, 12,661–12,675. https://doi.org/10.1029/2018JD029059

Barnston, A. G., & Livezey, R. E. (1987). Classification, seasonality and persistence of low-frequency atmospheric circulation patterns. *Monthly Weather Review*, *115*(6), 1083–1126. https://doi.org/10.1175/1520-0493(1987)115h1083:CSAPOLi2.0.CO;2

Barrett, B. S. (2019). Connections between the Madden-Julian Oscillation and surface temperatures in winter 2018 over eastern North America. *Atmospheric Science Letters*, *20*(1), e869. https://doi.org/10.1002/asl.869

Baxter, S., Weaver, S., Gottschalck, J., & Xue, Y. (2014). Pentad evolution of wintertime impacts of the Madden–Julian Oscillation over the contiguous United States. *Journal of Climate*, *27*(19), 7356–7367. https://doi.org/10.1175/JCLI-D-14-00105.1

Black, J., Johnson, N. C., Baxter, S., Feldstein, S. B., Harnos, D. S., & L'Heureux, M. L. (2017). The predictors and forecast skill of Northern Hemisphere teleconnection patterns for lead times of 3–4 weeks. *Monthly Weather Review*, *145*(7), 2855–2877. https://doi.org/10.1175/MWR-D-16-0394.1

Bladé, I., & Hartmann, D. L. (1995). The linear and nonlinear extratropical response of the atmosphere to tropical intraseasonal heating. *Journal of the Atmospheric Sciences*, *52*(24), 4448–4471. https://doi.org/10.1175/1520-0469(1995)052h4448:TLANERi2.0.CO;2

Bond, N. A., & Vecchi, G. A. (2003). The influence of the Madden-Julian Oscillation on precipitation in Oregon and Washington. *Weather and Forecasting*, *18*(4), 600–613. https://doi.org/10.1175/1520-0434(2003)018h0600:TIOTMOi2.0.CO;2

Cassou, C. (2008). Intraseasonal interaction between the Madden-Julian Oscillation and the North Atlantic Oscillation. *Nature*, *455*(7212), 523–527. https://doi.org/10.1038/nature07286

Curtis, S. (2017). The Madden-Julian Oscillation: A tool for regional seasonal precipitation outlooks? *Atmosphere*, *8*(9), 180 en. https://doi.org/10.3390/atmos8090180

Curtis, S., & Gamble, D. W. (2016). The boreal winter Madden-Julian Oscillation's influence on summertime precipitation in the Greater Caribbean. *Journal of Geophysical Research: Atmospheres*, *121*, 7592–7605. https://doi.org/10.1002/2016JD025031

DelSole, T., & Tippett, M. (2016). Forecast comparison based on random walks. *Monthly Weather Review*, *144*, 615–626. https://doi.org/10.1175/MWR-D-15-0218.1

DelSole, T., Trenary, L., Tippett, M. K., & Pegion, K. (2017). Predictability of week-3–4 average temperature and precipitation over the contiguous United States. *Journal of Climate*, *30*(10), 3499–3512. https://doi.org/10.1175/JCLI-D-16-0567.1

Donald, A., Meinke, H., Power, B., Maia, A. d. H. N., Wheeler, M. C., White, N., et al. (2006). Near-global impact of the Madden-Julian Oscillation on rainfall. *Geophysical Research Letters*, *33*, L09704. https://doi.org/10.1029/2005GL025155

Goss, M., & Feldstein, S. B. (2015). The impact of the initial flow on the extratropical response to Madden–Julian Oscillation convective heating. *Monthly Weather Review*, *143*(4), 1104–1121. https://doi.org/10.1175/MWR-D-14-00141.1

Guo, Y., Shinoda, T., Lin, J., & Chang, E. K. M. (2017). Variations of Northern Hemisphere storm track and extratropical cyclone activity associated with the Madden-Julian Oscillation. *Journal of Climate*, *30*(13), 4799–4818. https://doi.org/10.1175/JCLI-D-16-0513.1

Henderson, S. A., Maloney, E. D., & Barnes, E. A. (2016). The influence of the Madden-Julian Oscillation on Northern Hemisphere winter blocking. *Journal of Climate*, *29*(12), 4597–4616. https://doi.org/10.1175/JCLI-D-15-0502.1

Henderson, S. A., Maloney, E. D., & Son, S. W. (2017). Madden-Julian Oscillation Pacific teleconnections: The impact of the basic state and MJO representation in general circulation models. *Journal of Climate*, *30*(12), 4567–4587. https://doi.org/10.1175/JCLI-D-16-0789.1

Higgins, R. W., & Mo, K. C. (1997). Persistent North Pacific circulation anomalies and the tropical intraseasonal oscillation. *Journal of Climate*, *10*(2), 223–244. https://doi.org/10.1175/1520-0442(1997)010h0223:PNPCAAi2.0.CO;2

Hoskins, B. J., & Ambrizzi, T. (1993). Rossby wave propagation on a realistic longitudinally varying flow. *Journal of the Atmospheric Sciences*, *50*(12), 1661–1671. https://doi.org/10.1175/1520-0469(1993)050h1661:RWPOARi2.0.CO;2

Jenney, A. M., Randall, D. A., & Barnes, E. A. (2019). Quantifying regional sensitivities to periodic events: Application to the MJO. *Journal of Geophysical Research: Atmospheres*, *124*, 3671–3683. https://doi.org/10.1029/2018JD029457

Johnson, N. C., Collins, D. C., Feldstein, S. B., L'Heureux, M. L., & Riddle, E. E. (2014). Skillful wintertime North American temperature forecasts out to 4 weeks based on the state of ENSO and the MJO*. *Weather and Forecasting*, *29*(1), 23–38. https://doi.org/10.1175/WAF-D-13-00102.1

Jones, C., Gottschalck, J., Carvalho, L. M. V., & Higgins, W. (2011). Influence of the Madden-Julian Oscillation on forecasts of extreme precipitation in the contiguous United States. *Monthly Weather Review*, *139*(2), 332–350. https://doi.org/10.1175/2010MWR3512.1

Kalkstein, L. S., & Smoyer, K. E. (1993). The impact of climate change on human health: Some international implications. *Experientia*, *49*(11), 969–979. en. https://doi.org/10.1007/BF02125644

Kalnay, E., Kanamitsu, M., Kistler, R., Collins, W., Deaven, D., Gandin, L., et al. (1996). The NCEP/NCAR 40-year reanalysis project. *Bulletin of the American Meteorological Society*, *77*(3), 437–472. https://doi.org/10.1175/1520-0477(1996)077h0437:TNYRPi2.0.CO;2

Kang, W., & Tziperman, E. (2018). The MJO-SSW teleconnection: Interaction between MJO-forced waves and the midlatitude jet. *Geophysical Research Letters*, *45*, 4400–4409. https://doi.org/10.1029/2018GL077937

Kiladis, G. N., Dias, J., Straub, K. H., Wheeler, M. C., Tulich, S. N., Kikuchi, K., et al. (2014). A comparison of OLR and circulation-based indices for tracking the MJO. *Monthly Weather Review*, *142*(5), 1697–1715. https://doi.org/10.1175/MWR-D-13-00301.1

Lee, Y.-Y., & Grotjahn, R. (2019). Evidence of specific MJO phase occurrence with summertime California Central Valley extreme hot weather. *Advances in Atmospheric Sciences*, *36*(6), 589–602. https://doi.org/10.1007/s00376-019-8167-1

Lin, H. (2009). Global extratropical response to diabatic heating variability of the Asian summer monsoon. *Journal of the Atmospheric Sciences*, *66*(9), 2697–2713. https://doi.org/10.1175/2009JAS3008.1

Lin, H., Brunet, G., & Fontecilla, J. S. (2010). Impact of the Madden-Julian Oscillation on the intraseasonal forecast skill of the North Atlantic Oscillation. *Geophysical Research Letters*, *37*, L19803. https://doi.org/10.1029/2010GL044315

Lin, H., Brunet, G., & Mo, R. (2010). Impact of the Madden-Julian Oscillation on wintertime precipitation in Canada. *Monthly Weather Review*, *138*(10), 3822–3839. https://doi.org/10.1175/2010MWR3363.1

Lorenz, D. J., & Hartmann, D. L. (2006). The effect of the MJO on the North American monsoon. *Journal of Climate*, *19*(3), 333–343. https://doi.org/10.1175/JCLI3684.1

Matsueda, S., & Takaya, Y. (2015). The global influence of the Madden–Julian Oscillation on extreme temperature events. *Journal of Climate*, *28*, 4141–4151. https://doi.org/10.1175/JCLI-D-14-00625.1

McKinnon, K. A., Rhines, A., Tingley, M. P., & Huybers, P. (2016). Long-lead predictions of eastern United States hot days from Pacific sea surface temperatures. *Nature Geoscience*, *9*(5), 389–394. https://doi.org/10.1038/ngeo2687

Menne, M. J., Durre, I., Vose, R. S., Gleason, B. E., & Houston, T. G. (2012). An overview of the global historical climatology network-daily database. *Journal of Atmospheric and Oceanic Technology*, *29*(7), 897–910. https://doi.org/10.1175/JTECH-D-11-00103.1

Mo, K. C. (2000). Intraseasonal modulation of summer precipitation over North America. *Monthly Weather Review*, *128*(5), 1490–1505. https://doi.org/10.1175/1520-0493(2000)128h1490:IMOSPOi2.0.CO;2

Moon, J.-Y., Wang, B., Ha, K.-J., & Lee, J.-Y. (2013). Teleconnections associated with Northern Hemisphere summer monsoon intraseasonal oscillation. *Climate Dynamics*, *40*(11), 2761–2774. https://doi.org/10.1007/s00382-012-1394-0

Moore, R. W., Martius, O., & Spengler, T. (2010). The modulation of the subtropical and extratropical atmosphere in the Pacific basin in response to the Madden-Julian Oscillation. *Monthly Weather Review*, *138*(7), 2761–2779. https://doi.org/10.1175/2010MWR3194.1

Mori, M., & Watanabe, M. (2008). The growth and triggering mechanisms of the PNA: A MJO-PNA coherence. *Journal of the Meteorological Society of Japan*, *86*(1), 213–236. https://doi.org/10.2151/jmsj.86.213

Mundhenk, B. D., Barnes, E. A., Maloney, E. D., & Baggett, C. F. (2018). Skillful empirical subseasonal prediction of landfalling atmospheric river activity using the Madden–Julian Oscillation and Quasi-Biennial Oscillation. *Npj Climate and Atmospheric Science*, *1*(1), 7. https://doi.org/10.1038/s41612-017-0008-2

Newman, M., & Sardeshmukh, P. D. (1998). The impact of the annual cycle on the North Pacific/North American response to remote low-frequency forcing. *Journal of the Atmospheric Sciences*, *55*(8), 1336–1353. https://doi.org/10.1175/1520-0469(1998)055h1336:TIOTACi2.0.CO;2

Rodney, M., Lin, H., & Derome, J. (2013). Subseasonal prediction of wintertime North American surface air temperature during strong MJO events. *Monthly Weather Review*, *141*(8), 2897–2909. https://doi.org/10.1175/MWR-D-12-00221.1

Sardeshmukh, P. D., & Hoskins, B. J. (1988). The generation of global rotational flow by steady idealized tropical divergence. *Journal of Atmospheric Sciences*, *45*(7), 1228–1251. https://doi.org/10.1175/1520-0469(1988)045h1228:TGOGRFi2.0.CO;2

Schreck, C. J., Cordeira, J. M., & Margolin, D. (2013). Which MJO events affect North American temperatures? *Monthly Weather Review*, *141*(11), 3840–3850. https://doi.org/10.1175/MWR-D-13-00118.1

Seo, K.-H., Lee, H.-J., Seo, K.-H., & Lee, H.-J. (2017). Mechanisms for a PNA-like teleconnection pattern in response to the MJO. *Journal of the Atmospheric Sciences*, *74*(6), 1767–1781. https://doi.org/10.1175/JAS-D-16-0343.1

Seo, K.-H., & Son, S.-W. (2012). The global atmospheric circulation response to tropical diabatic heating associated with the Madden–Julian Oscillation during northern winter. *Journal of the Atmospheric Sciences*, *69*(1), 79–96. https://doi.org/10.1175/2011JAS3686.1

Simmons, A. J., Wallace, J. M., & Branstator, G. W. (1983). Barotropic wave propagation and instability, and atmospheric teleconnection patterns. https://doi.org/10.1175/1520-0469(1983)040h1363:BWPAIi2.0.CO;2

Stan, C., Straus, D. M., Frederiksen, J. S., Lin, H., Maloney, E. D., & Schumacher, C. (2017). Review of tropical-extratropical teleconnections on intraseasonal time scales: The subseasonal to seasonal (S2S) teleconnection Sub-Project. *Reviews of Geophysics*, *55*, 902–937. https://doi.org/10.1002/2016RG000538

Ting, M., & Sardeshmukh, P. D. (1993). Factors determining the extratropical response to equatorial diabatic heating anomalies. *Journal of the Atmospheric Sciences*, *50*(6), 907–918. https://doi.org/10.1175/1520-0469(1993)050h0907:FDTERTi2.0.CO;2

Tseng, K.-C., Maloney, E., & Barnes, E. (2019). The consistency of MJO teleconnection patterns: An explanation using linear Rossby wave theory. *Journal of Climate*, *32*(2), 531–548. https://doi.org/10.1175/JCLI-D-18-0211.1

Wang, L., Li, T., Zhou, T., & Rong, X. (2013). Origin of the intraseasonal variability over the North Pacific in boreal summer. *Journal of Climate*, *26*(4), 1211–1229. https://doi.org/10.1175/JCLI-D-11-00704.1

Wang, S., Ma, D., Sobel, A. H., & Tippet, M. K. (2018). Propagation characteristics of BSISO indices. *Geophysical Research Letters*, *45*, 9934–9943. https://doi.org/10.1029/2018GL078321

Wang, B., & Rui, H. (1990). Synoptic climatology of transient tropical intraseasonal convection anomalies: 1975–1985. *Meteorology and Atmospheric Physics*, *44*(1), 43–61. https://doi.org/10.1007/BF01026810

Wang, S., Sobel, A. H., Tippett, M. K., & Vitart, F. (2019). Prediction and predictability of tropical intraseasonal convection: Seasonal dependence and the Maritime Continent prediction barrier. *Climate Dynamics*, *52*(9), 6015–6031. https://doi.org/10.1007/s00382-018-4492-9

Wheeler, M. C., & Hendon, H. H. (2004). An all-season real-time multivariate MJO index: Development of an index for monitoring and prediction. *Monthly Weather Review*, *132*(8), 1917–1932. https://doi.org/10.1175/1520-0493(2004)132h1917:AARMMIi2.0.CO;2

White, C. J., Carlsen, H., Robertson, A. W., Klein, RichardJ. T., Lazo, J. K., Kumar, A., et al. (2017). Potential applications of subseasonal-to-seasonal (S2S) predictions. *Meteorological Applications*, *24*(3), 315–325. https://doi.org/10.1002/met.1654

Wilks, D. S. (2011). Statistical methods in the atmospheric sciences. https://doi.org/10.1016/B978-0-12-385022-5.00026-9

Zhang, C. (2013). Madden-Julian Oscillation: Bridging weather and climate. *Bulletin of the American Meteorological Society*, *94*(12), 1849–1870. https://doi.org/10.1175/BAMS-D-12-00026.1

Zheng, C., Kar-Man Chang, E., Kim, H.-M., Zhang, M., & Wang, W. (2018). Impacts of the Madden–Julian Oscillation on storm-track activity, surface air temperature, and precipitation over North America. *Journal of Climate*, *31*(15), 6113–6134. https://doi.org/10.1175/JCLI-D-17-0534.1

Zhou, S., L'Heureux, M., Weaver, S., & Kumar, A. (2012). A composite study of the MJO influence on the surface air temperature and precipitation over the continental United States. *Climate Dynamics*, *38*(7-8), 1459–1471. https://doi.org/10.1007/s00382-011-1001-9